Numerical Study of How the Ground Shock Coupling Factor is Influenced by Soil Properties

Leo Laine[a,*] and Ola Pramm Larsen[b]

[a]ANKER – ZEMER Engineering A/S
Stugvägen 4, SE-438 94 HÄRRYDA, Sweden
[*]Corresponding author: leo.laine@telia.com

[b]ANKER – ZEMER Engineering A/S
P.O. Box 253, NO-0702 OSLO, Norway

Already during the Second World War empirical expressions were derived to predict the magnitude and impulse of a ground shock generated by high explosives. One parameter that is of main importance when using the empirical equations is the coupling factor. The coupling factor describes how much of the released energy from the high explosive is transmitted into the ground as a function of depth of burial. This paper aims to clarify which soil properties influence the coupling factor as a function of the scaled depth of explosion. The ground shock was analysed with a two-dimensional axis symmetric explicit finite element solver with a multi-material euler formulation. A total of 4 different soil materials were analysed, scaling from dry sand to fully saturated clay. The scaled depth of burial was varied between -0.1 to 1.0 m/kg$^{1/3}$. Targets points in horizontal, vertical and 45 degree angle direction were used to derive the coupling factor by applying the analysed results of peak pressure and particle velocity. The simulation results were compared with the generalised coupling factor found in the ground shock literature. According to the literature the generalised coupling factor increases smoothly with reduced derivative as function of depth of burial. The same generic function is mainly proposed to be used for all loose soils. The simulation results indicate that the coupling factor must be seen as a more complicated relationship than only dependent on depth of burial. The simulation results showed that it will vary with; the soil properties, studied angle from the centre of explosive, and the scaled distance from the explosive. Additionally, for dry sand the coupling factor curve showed an unexpected minimum at 0.05 m/kg$^{1/3}$ depth of burial for the studied results in 45 degree angle.

INTRODUCTION

The Swedish Rescue Services Agency (SRSA) is responsible for the building regulations of the Swedish civil defence shelters. The shelters have specific regulations for how they are planned, built, equipped and maintained [1]. One of many regulations state what loading level the shelters should withstand: “The effect of a pressure wave corresponding to that produced by a 250 kg GP-bomb with 50 weight per cent TNT which burst freely outside at a distance of 5.0 meters from the outside of the shelter during free pressure release”. However, many of the shelters are designed as basements below ground surface. This is the reason why more knowledge about how the shock wave affects buried shelters is needed.

During the Second World War extensive experiment series and research were conducted on ground shock generated by high explosives [2]. This early work functions as a foundation for the empirical equations that are widely used to

estimate the loading from ground shock [3]-[6]. There is especially one parameter in these empirical equations that is very important for the accuracy of the empirical equations, and that is the coupling factor. The coupling factor *f* is described in [4] by the following relationship

$$f = \frac{(p, u_p, d_p, i, a)_{\text{near surface}}}{(p, u_p, d_p, i, a)_{\text{contained}}} \qquad \text{(eq.1)}$$

where the numerator represents the ground shock magnitudes of a partially to shallow buried explosive and the denominator represents the magnitude of a fully buried explosive in the same medium. The ground shock magnitudes in eq.1 are pressure *p,* particle velocity u_p, particle displacement d_p, impulse *i,* and acceleration *a.* The validity range of eq.1 is given from 0.8 m/kg$^{1/3}$ to 5.0 m/kg$^{1/3}$. In the literature, [3]-[5], it is often shown that the coupling factor *f*(*d*) is a function of scaled depth of burial *d* and can be generalised as one smooth slowly increasing *f*(*d*) curve that represent loose soils, see Fig 1. The aim of this paper was to find out if this generalised *f*(*d*) curve can be verified by numerical simulations and if the shape of the curve varies with other parameters than only the depth of burial.

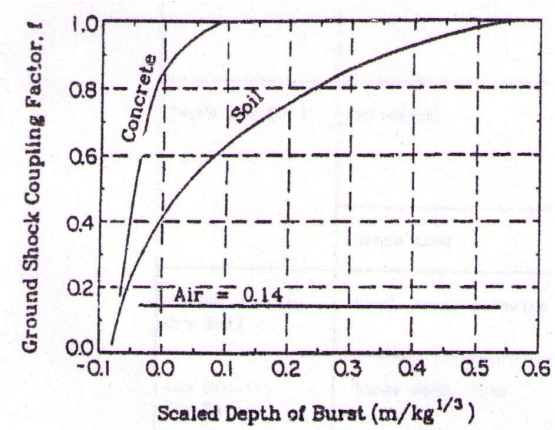

Fig. 1. Ground shock Coupling Factor *f* as a function of scaled depth of burst *d*. Figure originally from [4].

The outline of the paper is as follows: The section FINITE ELEMENT MODEL is discussing how the model was setup. Section SOIL MATERIALS shows how the different soil properties were generated. In SIMULATIONS section the analyses and results are shown. Finally, CONCLUSIONS section concludes the findings.

FINITE ELEMENT MODEL

The finite element model has been designed to capture how the scaled depth of burial *d*, scaled distances to the charge at various angles, and the soil properties, affect the magnitudes of the shock wave in the ground. The shock propagation was analysed with a two dimensional axis symmetric explicit finite element solver with multi-material Euler formulation found in AUTODYN^{TM} [7]. The charge was modelled with the Jones-Wilkins-Lee Equation Of State (EOS) and the used explosive charge weight was 1 kg TNT. The air was modelled as ideal gas. The scaled *d* was varied between -0.1 to 1 kg/m$^{1/3}$. The shock wave magnitudes were studied at different scaled distances from the charge in three different angular directions in the soil. The studied angle directions were horizontal, -45 degrees downward, and -90 degrees vertically downward, see Fig. 2.

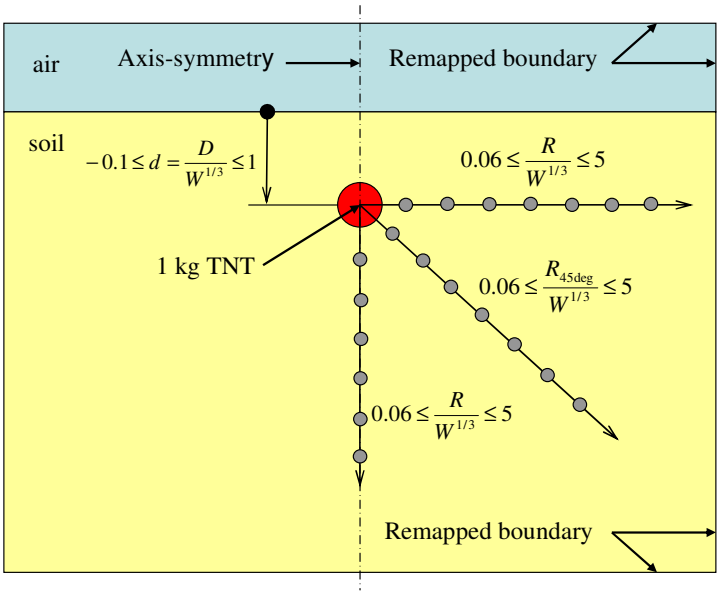

Fig. 2. Principal layout of the finite element model. The red area illustrates the explosive with scaled depth of burial $d = D/W^{1/3}$, where D is the depth of burial. The gray dots illustrate target points used to measure ground shock magnitude parameters.

Usually, when euler models are built, boundaries of type outflow or transmit are used to limit the lengths and number of used cells. However, these boundaries are only approximations and introduce numerical errors and therefore are required to be sufficiently far from the studied area to ensure accuracy in the simulations. Such error sources, though, were avoided in the analyses by using an automated remapping functionality that expanded the lengths of the euler domain with the ratio 2:1 during each remap. The used number of cells of the domains was kept constant, 400x200, see Fig 3. The remapping was done just before the shock wave reached the end of the domain. The automation was implemented in AUTODYN by using a combination of scripting macros and user-subroutines.

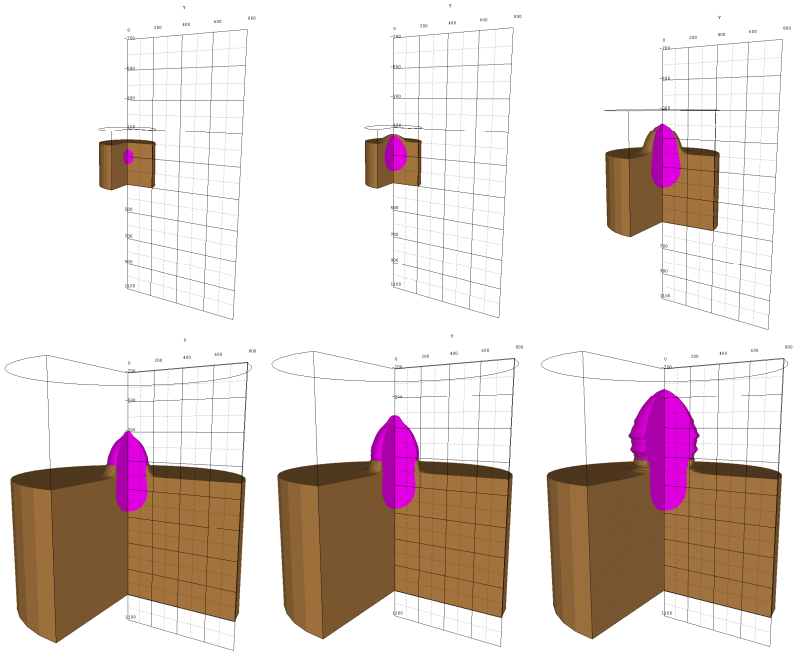

Fig. 3. Illustration of when the euler domain is expanded by using remapping. Upper left material location plot shows when the domain is the smallest and then some of the expanded domains. The purple and brown colours illustrate the expanding high explosive gases and the soil, respectively

SOIL MATERIALS

The soil material properties were gradually changed from dry sand to fully saturated clay. A total of 4 different soil materials were generated to study the effect of the coupling factor. In this study, the material model used was derived to study granular materials [8]. When deriving the generic soil materials in-between the two extremes, dry sand and fully saturated clay, their Equation Of States (EOS) and strength parameters were selected as starting and ending curves. The starting EOS was the dry sand found in [9]-[10], here named E1 the second EOS was for a fully saturated clay, here named E4. Linear scaling was used to derive two more EOS between these two extremes named E2 and E3. The gradual scaling of EOS is shown in Fig. 4. Similarly the shear strength was linearly scaled between the dry sand [9]-[10] and the fully saturated clay to generate S1, S2, S3, and S4 respectively as illustrated in Fig. 5.

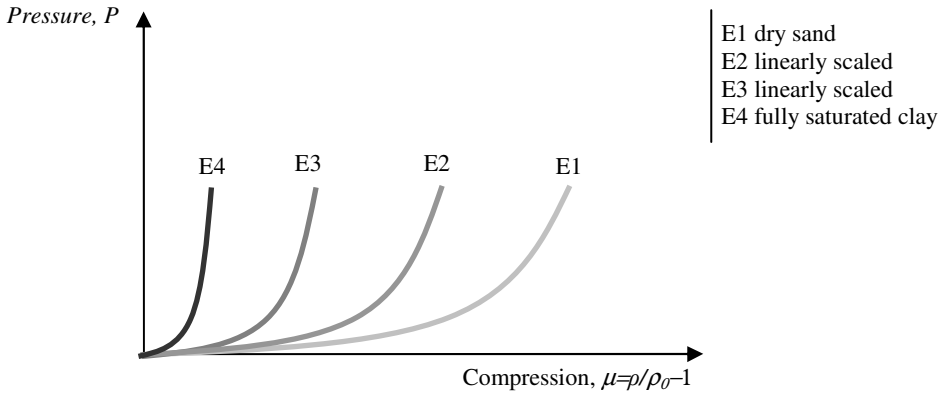

Fig. 4. Illustration of how the Equation of State, Ei, is varying for the different soils and the linear scaling between the dry sand and the fully saturated clay.

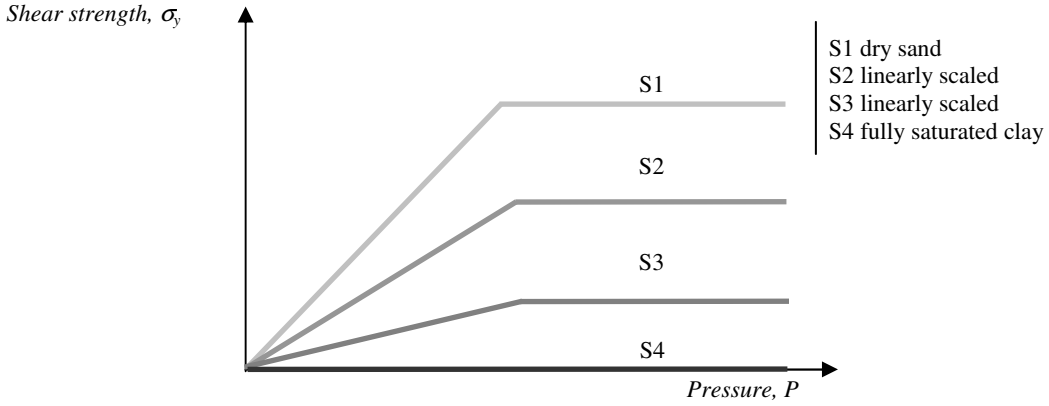

Fig. 5. Illustration of how the shear strength, Si, is varying for the various soils and the linear scaling between the dry sand and the fully saturated clay.

The material model allows the user to define the EOS as pressure as a function of density $P(\rho)$, shear strength as a function of pressure $\sigma_y(P)$, bulk sound speed as a function of density $c(\rho)$, and finally shear modulus as a function of density $G(\rho)$. Each one of the soil properties required their specific $c(\rho)$ and $G(\rho)$. Additionally a hydro tensile limit of P_{min} = -1 kPa was defined for all soil properties due to the soils lack of handling any negative pressure on a macro level.

The studied soil materials E1-S1 (dry sand), E2-S2, E3-S3, and E4-S4 (fully saturated clay) and their material properties are found in [11]. Only the properties of dry sand, E1-S1, are based on experimental data [9]-[10]. These experiments were performed on sand found in Sjöbo, Sweden. In these experiments, tri-axial pressure cells up to about 100 MPa were used. The tests were performed first by isotropical loading and unloading to receive a fairly

good picture of the porous EOS. The experiments were followed by tri-axial shear tests. Additionally the pressure and shear waves were measured during the tests by P- and S- transducers to get an idea how the bulk modulus and shear modulus varies with density and pressure. The fully saturated clay is only a generic soil property, similar to what is found in shock literature, of what could be expected by fully saturated clay.

SIMULATIONS

The simulations were performed in such a way that every analysis had a different scaled depth of burial d for the explosive charge. The parameter d was varied with following steps d = [-0.1, -0.05, 0, 0.05, 0.1, 0.15, 0.2, 0.3, 0.4, 0.5, 0.6, 0.8, 1] m/kg$^{1/3}$. This was done for all four soil materials, which gives a total of 4x13 = 52 simulations. To derive the coupling factor the simple relationship presented in eq.1 is used. Fig. 6 shows the calculated coupling factor based upon maximum pressure for scaled charge distance $Z = R/W^{1/3}$ = 3.69 m/kg$^{1/3}$ and angle of -45 degrees for the studied soil properties. However, from this it is hard to distinguish any clear trends for the coupling factor based on the maximum pressure for the different soil properties. Some general trends can be seen for the soil properties as group, the coupling factor becomes close to $f \rightarrow 1$ for all soil properties when scaled depth of burial comes closer to $d \rightarrow 0.6$. This trend is also what is used in the literature, see Fig. 1. Another major trend is that all soil properties except for sand have generally increasing coupling factor with increasing scaled depth of burial.

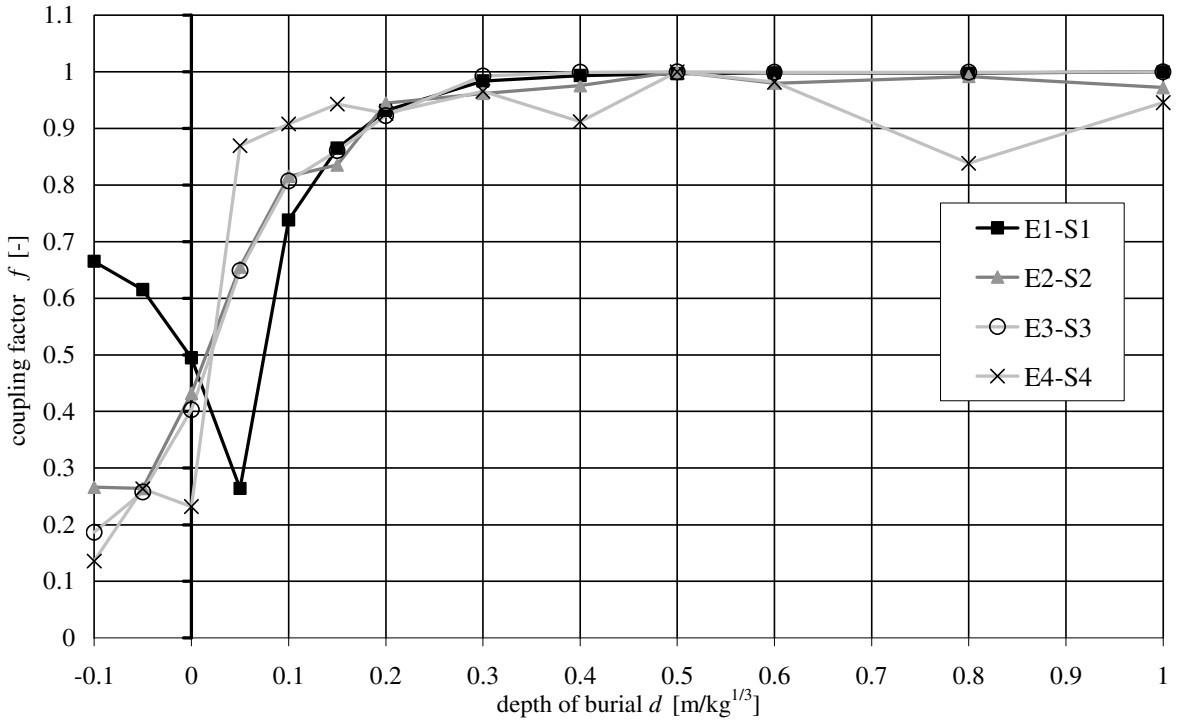

Fig. 6. Coupling factor f as a function of depth of burial d for the scaled distance Z = 3.69 m/kg$^{1/3}$ and angle -45 degrees for the four soil properties.

By continuing to study the maximum pressure based coupling factor f and studying how the target angle affects the results for one of the soil properties, a clear trend is apparent, the coupling factor function starts at a higher level and its derivative becomes higher when the target angle moves from 0 to -45 to -90 degrees. In Fig. 7 this is illustrated for one of the generic soil properties E3-S3 which can represent the general trend for all soils.

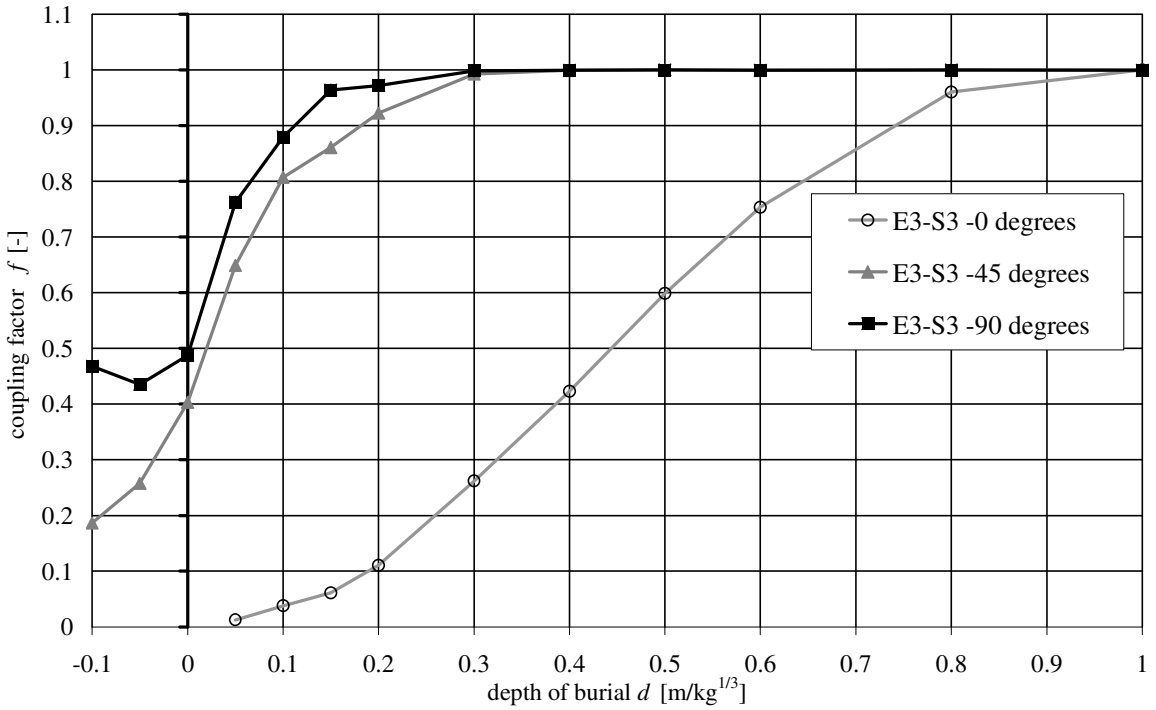

Fig. 7. Coupling factor f as a function of depth of burial d for the scaled distance Z = 3.69 m/kg$^{1/3}$ and angle 0, -45, and -90 degrees for the soil property E3-S3.

A similar trend is also observed when different target distances are studied as shown in Fig 8. The coupling factor function receives a steeper derivative when the scaled distance to target Z is reduced.

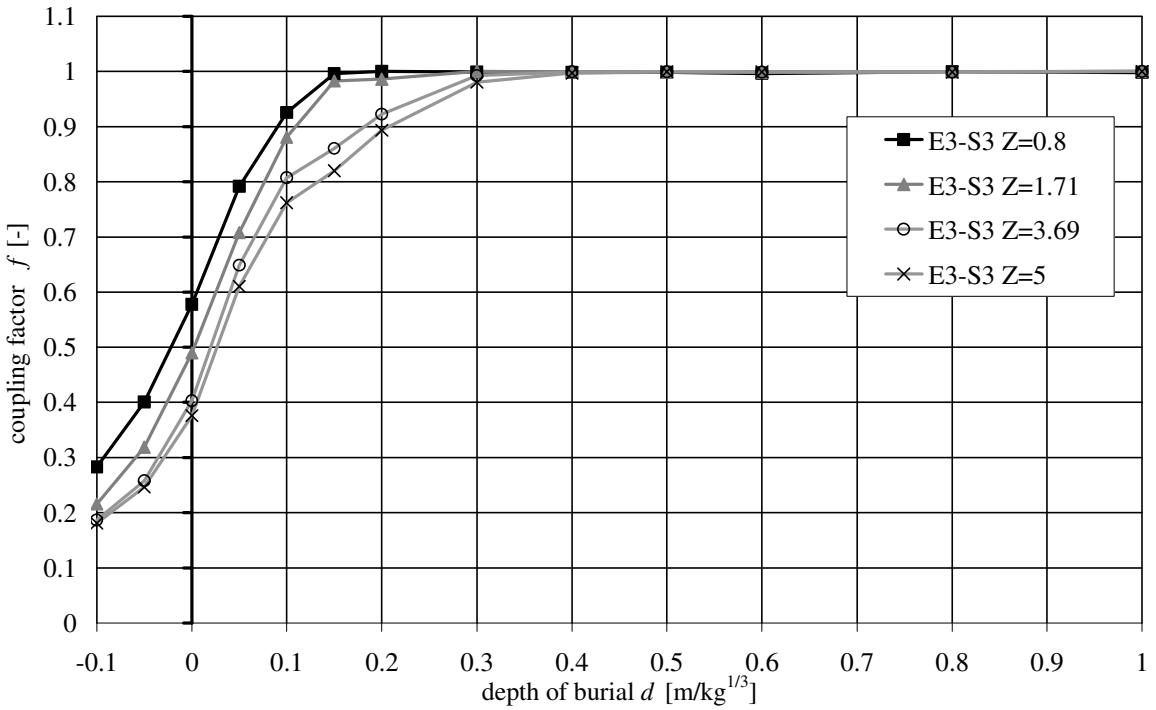

Fig. 8. Coupling factor f as a function of depth of burial d for the scaled distances Z = 0.8, 1.71, 3.69, and 5 m/kg$^{1/3}$ and angle -45 degrees for the soil property E3-S3.

An interesting phenomenon was observed for the dry sand, E1-S1, for the target angle -45 degrees. It actually showed that a minimum occurred for the coupling function f not at depth of burial -0.1 m/kg$^{1/3}$ as expected instead it occurred at +0.05 m/kg$^{1/3}$, see Fig. 9.

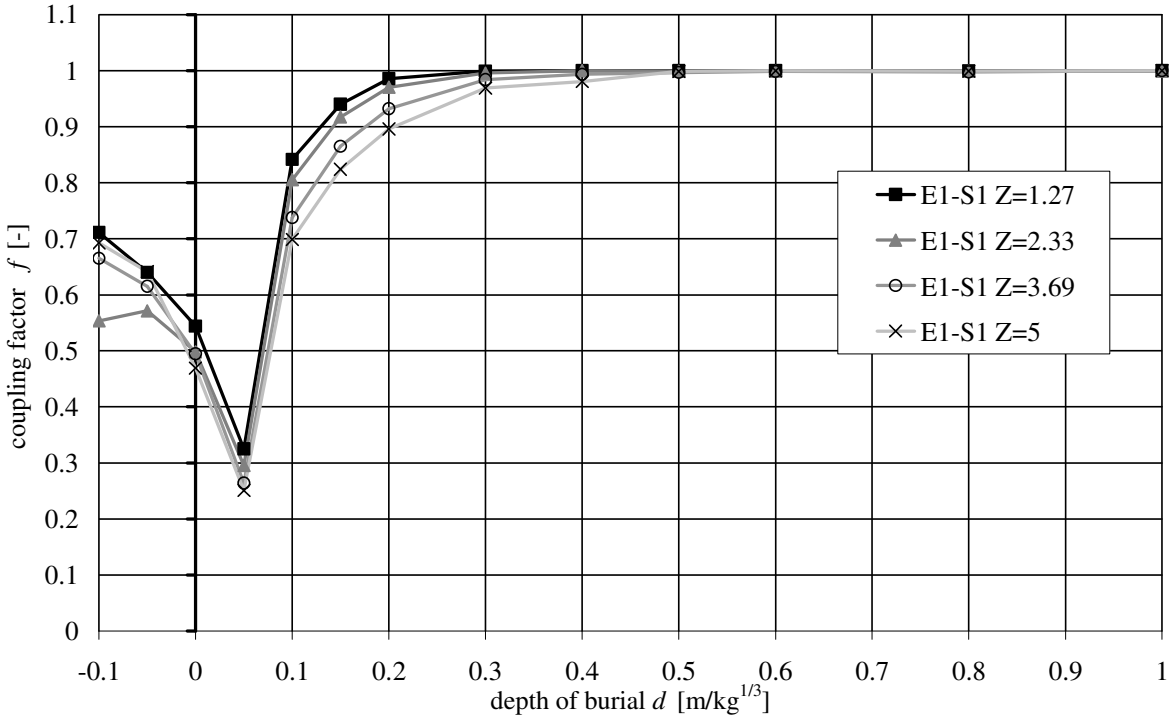

Fig. 9. Coupling factor f as a function of depth of burial d for the scaled distances Z = 1.27, 2.33, 3.69, and 5 m/kg$^{1/3}$ and angle -45 degrees for the soil property dry sand E1-S1.

The phenomenon with a transferred minimum point can be explained by studying the pressure propagation for depth of burial d = -0.1 m/kg$^{1/3}$ and d = 0.05 m/kg$^{1/3}$ for a target point in the -45 degree angle, see Fig. 10 and Fig. 11, respectively. It can be seen, that when the charge is above ground, d = -0.1 m/kg$^{1/3}$, the shock wave propagates faster in air than in the ground. The E1-S1 has the slowest sound speed of all the studied soil materials. This gives the effect of that the airblast actually initiate a shock wave in the soil before the pure ground shock has reached the studied surface point. This gives an un-symmetric propagation of the ground shock and explains why an increase in the coupling factor occurs when the charge is in the air. In Fig. 11 it is seen that when the charge is slightly buried, d = 0.05 m/kg$^{1/3}$, the un-symmetric behaviour is almost totally disappeared. This is due to the fact that the airblast is weakened along the horizontal direction.

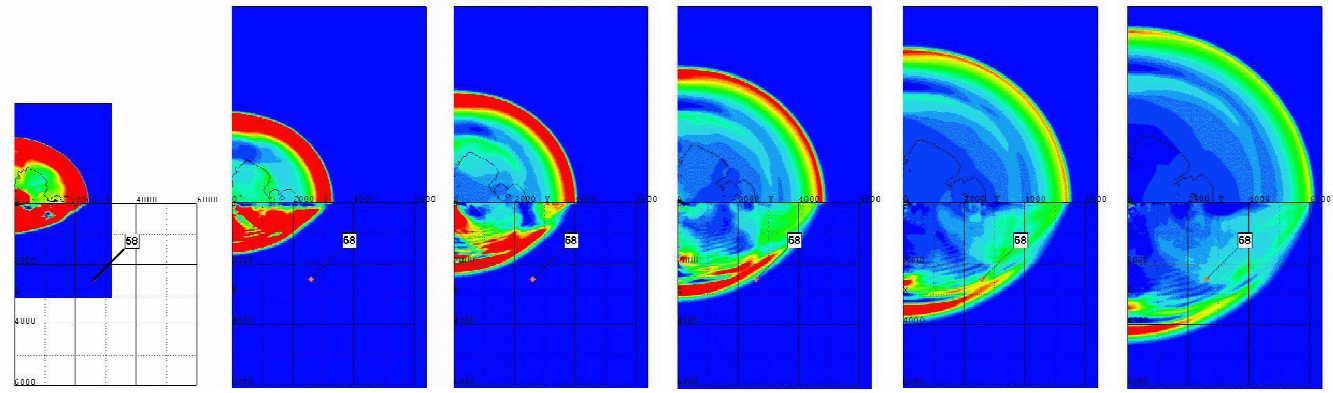

Fig. 10. Pressure plots at times 2, 4, 6, 8, 10, and 12 ms for the soil property dry sand E1-S1 with depth of burial d = -0.1 m/kg$^{1/3}$. Red colour corresponds to 40 kPa or higher and blue to 0 kPa. 58 is a 45 degree angle target point.

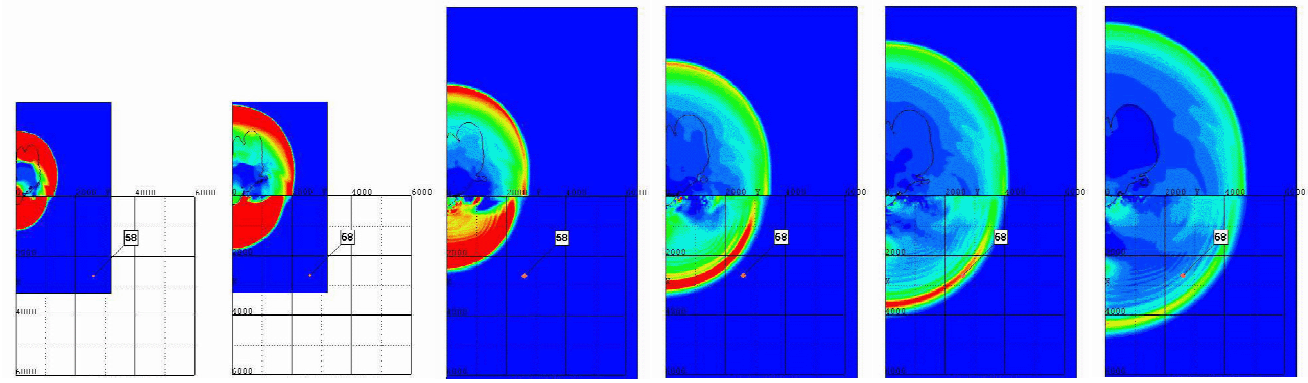

Fig. 11. Pressure plots at times 2, 4, 6, 8, 10, and 12 ms for the soil property dry sand E1-S1 with depth of burial d = +0.05 m/kg$^{1/3}$. Red colour corresponds to 40 kPa or higher and blue to 0 kPa. 58 is a 45 degree angle target point.

The calculated coupling factor based upon maximum particle velocity did not differentiate much from the case when maximum pressure was used. The results from these plots are therefore omitted from this paper. Eq.1 also suggests impulse to be used to derive the coupling factor. The simulation results showed that when the impulse was used a general trend was that the coupling factor f became in significantly lower and not so steep slope compared with pressure and particle based coupling factor. Another issue with using impulse are the reflections which occur from the surface. These surface reflections will influence and reduce the impulse results for scaled distances that are of interest, ranging from 0.8 m/kg$^{1/3}$ to 5.0 m/kg$^{1/3}$. Maximum accelerations are hard to receive correct measurements of in field tests and are therefore excluded here. However, when the coupling factor was calculated by using the ratio of kinetic energy transferred to the soil and to the air, a clear distinction could be seen in the coupling factor function when the different soil properties were studied, see Fig. 12. The Fig. 12 was derived by studying the ratio of air kinetic energy and soil kinetic energy at analysis time 3 ms. Adjustments on the kinetic energy curves were needed due to jumps when remapping was performed. The jumps occur because some of the soil ejecta are not remapped correctly and these high kinetic energy parts of the soil are excluded from the calculation, this gives a clear instant loss when remapping is performed. But with the adjustments, by adding the kinetic energy jump after each remap, the curve became smooth over the whole analysis time. The results of Fig. 12 show that the clay is clearly faster than the other soils in reaching the full coupling factor of f=1 when depth of burial d is increased. For example at d=0 m/kg$^{1/3}$ the sand has only f=0.19 and the clay has f=0.47m which is an increase in 147 percent. At d=0.05 m/kg$^{1/3}$ the sand has a coupling factor of f=0.64 and the clay has f=0.73m which is an increase in 14 percent. This indicates the need of including the soil type and its properties in the definition of the coupling factor.

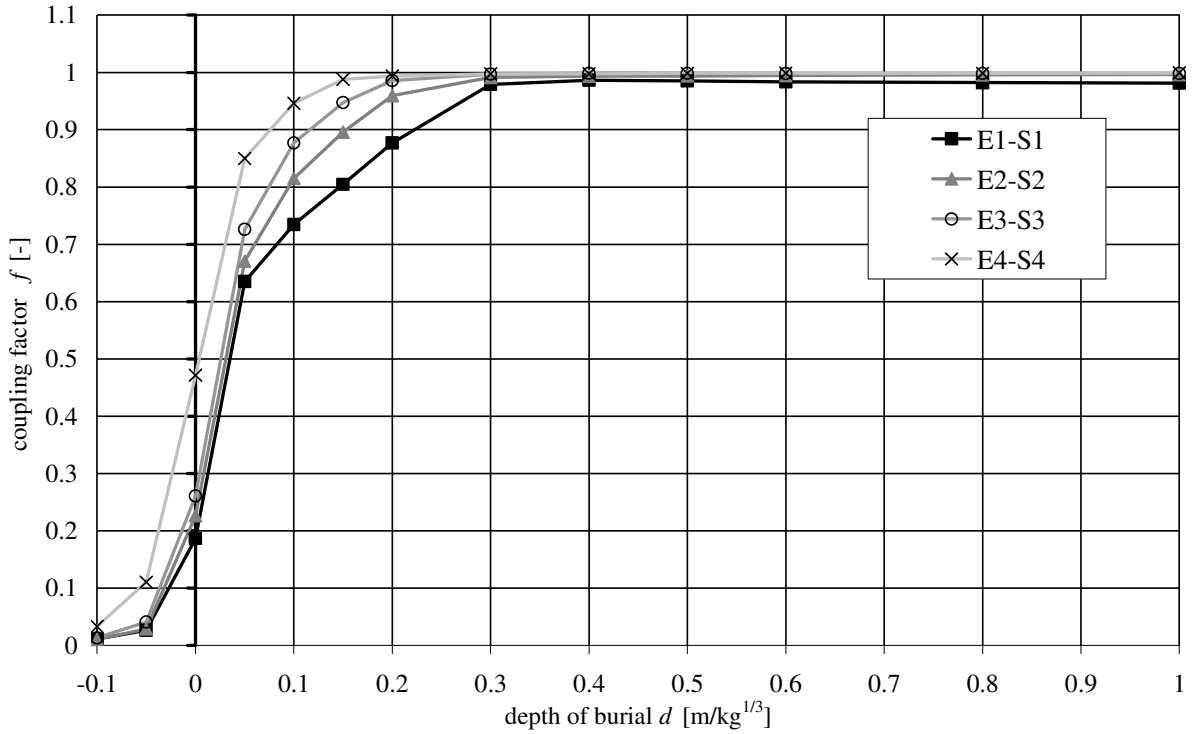

Fig. 12. Coupling factor f based upon transferred ratio of kinetic energy $f = E_{k,soil}/E_{k,total}$ for the four soil properties as a function of scaled depth of burial at analysis time 3ms.

CONCLUSIONS

The paper's objectives of finding clear relationships of what soil properties influence the coupling factor was not fulfilled. The results presented here indicate that the coupling factor is not only influenced by the scaled depth of burial but it is also influenced by the soil properties, as expected. The influence of the soil properties on the coupling factor was though already acknowledged by [2] but somehow it became accepted to utilize a simplified coupling factor in the following years, 1946-1989. However, this paper indicates that the coupling factor is also influenced by the geometrical layout of the studied problem. This combined effect makes it harder to draw any clear conclusions therefore only some observations and argumentations can be stated at this point:

1. The soil properties have an influence of how steep the coupling factor is as a function of depth of burial. This is clearly seen when studying the ratio of kinetic energy transmitted to soil and air. The soil material which has the most porous equation of state resulted in the weakest coupling factor function. The derivative of the coupling factor function seemed to increase when the equation of state became less porous, see also Fig 11. This indicate that different coupling factor functions should be used for different loose soils or at least incorporate a scaling parameter based upon soil properties on the general coupling factor function.

2. When studying the coupling factor function by calculating it by using maximum pressure or particle velocity it can be seen that the scaled distance and the angle of the studied target locations are of influence. The results showed that when the scaled distance decreases the derivative of the coupling factor function increases and the coupling factor also receives a higher starting point. A corresponding effect seems to be present for the angle of the studied target locations.

3. An unexpected minimum on the coupling factor function was shown to occur for dry sand when the charge was shallow buried at 0.05 m/kg$^{1/3}$ and not when the charge was in the air, as expected and seen for the other studied soil properties. This minimum was clearly seen when -45 degree angle target locations with

different scaled distances were studied. The reason for this is that the charge detonating in air actually generated a ground shock wave with the airblast before the "pure ground shock" had reached a certain studied point on the surface. This is due to that the dry sand has much lower shock wave velocity than air. This result in a un-spherical shock wave propagation which is most likely is assumed to be spherical by the simple definition of the coupling factor found in [3], see eq.1. The validity range of scaled distance of 0.8 m/kg$^{1/3}$ to 5.0 m/kg$^{1/3}$ is specified which the FE analysis clearly show that nonspherical propagation will occur within this range.

4. Based on the large variations of the coupling factor relationship seen in the FE analysis when studying soils, different scaled distances, and target location angles, it is tempting to suggest an alternate coupling factor definition which is not dependent on local shock propagation properties to the same extent as the simple relationship suggests, see eq.1. Averaged quantities over the entire soil domain could probably be employed for yielding better consistency over the whole range of charge depths. Another suggested approach would be to use a global property like the kinetic energy distribution between soil and air, see Fig. 12. This approach would however be very hard to realize experimentally and is probably only feasible in a FE-analysis setting.

Finally, more studies of both experimental and simulative nature are encouraged to enlighten if a new definition of the coupling factor is needed and what main factors influence the shape of the coupling factor function in addition to the scaled depth of burial.

ACKNOWLEDGEMENTS

The authors acknowledge the support given by Swedish Rescue Services Agency and especially Björn Ekengren. Additionally members of the West Sweden Shock Wave Group and especially Dr. Morgan Johansson and Dr. Joosef Leppänen are highly acknowledged for their input. Finally, Jan-Christian Anker's feedback on the writing is highly appreciated.

REFERENCES

[1] Ekengren B. (2006): *Skyddsrum, SR 06 (Civil Shelters 06 in Swedish)*, Swedish Rescue Services Agency, B54-141/06, Karlstad, Sweden.
[2] Lampson C.W. (1946): Final Report on Effects of Underground Explosions, Div. 2, National Defence Research Committee of the US Office Scientific R&D, NDRC Report No. A-479, OSRD Report No. 6645.
[3] Drake J.L. och Little Jr C.D. (1983): Ground Shock from Penetrating Conventional Weapons, Interaction of Non-nuclear Munitions with Structures, U.S. Air Force Academy, USA.
[4] Drake J.L., Smith E. B., och Blouin S.E. (1989): Enhancements of the Prediction of Ground Shock from Penetrating Weapons, 4th Int. Symp. on the Interaction of Non-nuclear Munitions with Structures.
[5] Bulson P. (1997): Explosive Loading of Engineering Structures, ENFN SPON, London, England.
[6] ConWep (1992): Collection of conventional weapons effects calculations based on TM 5-855-1, Fundamentals of Protective Design for Conventional Weapons, U.S. Army Engineer Waterways Experiment Station, Vicksburg, USA.
[7] Century Dynamics Inc., (2004): *AUTODYN Theory Manual Revision 5.0*, San Ramon, CA, USA.
[8] Moxnes J. F., Ødegårdstuen G., Atwood A., and Curran P. (1999): "Mechanical properties of a porous material studied in a high speed piston driven compaction experiment", *30th International Annual Conference of ICT Energetic Materials, Fraunhofer Institut Chemische Technologie.*
[9] Laine L. and Sandvik A. (2001): "Derivation of mechanical properties for sand", *4th Asian-Pacific conference on Shock and Impact Loads on Structures*, CI-Premier PTE LTD, vol. 4, pp 353-360, Singapore.
[10] Heyerdahl H. and Madshus C. (2000): "EOS-data for sand, Tri-axial tests on sand from Sjöbo", Norges Geotekniske institutt, NGI rept. 20001157-1, Oslo, Norway.
[11] Laine L. (2006): "Study of Planar Ground Shock in Different Soils and Its Propagation Around a Rigid Block", 77th Shock and Vibration Symposium October, Monterey, CA.